

Energy-level diagrams of high-spin and low-spin molecules

H. De Raedt^{*1}, S. Miyashita², and K. Michielsen^{1,2}

¹ Department of Applied Physics-Computational Physics, Materials Science Centre,
University of Groningen, Nijenborgh 4, NL-9747 AG Groningen, The Netherlands

² Department of Applied Physics, Graduate School of Science, University of Tokyo, Bunkyo-ku,
Tokyo 113-8656, Japan

Received 1 September 2003, accepted 18 March 2004

Published online 14 April 2004

PACS 75.10.Jm, 75.45.+j, 75.50.Ee, 75.50.Xx

The magnetic energy-level diagrams for models of the Mn_{12} and V_{15} molecule are calculated using the Lanczos method with full orthogonalization and a Chebyshev-polynomial-based projector method. The effects of the Dzyaloshinskii-Moriya interaction on the appearance of energy-level repulsions and its relevance to the observation of steps in the time-dependent magnetization data are studied.

© 2004 WILEY-VCH Verlag GmbH & Co. KGaA, Weinheim

1 Introduction

Magnetic molecules such as Mn_{12} or V_{15} have attracted a lot of interest recently because these nanomagnets can be used to study e.g. quantum (de)coherence, relaxation and tunneling of the magnetization on a nanoscale [1–22]. As a result of the very weak intramolecular interactions between these molecules, experiments directly probe the magnetization dynamics of the individual molecules. In particular the adiabatic change of the magnetization at low-temperature is governed by the discrete energy-level structure [23–26]. As the magnetization dynamics of these molecules is determined by the (tiny) level repulsions, a detailed knowledge of the low-lying energy level scheme is necessary.

Magnetic anisotropy, a result of the geometrical arrangement of the magnetic ions within a molecule of low symmetry, mixes states of different total spin and enforces a treatment of the full Hilbert space of the system. Disregarding the single-ion anisotropy, the dominant contribution to the magnetic anisotropy due to spin-orbit interactions is given by the Dzyaloshinskii-Moriya interaction (DMI) [27–33]. In principle this interaction can change energy-level crossings into energy-level repulsions. The presence of the latter is essential to explain the adiabatic changes of the magnetization at the resonant fields in terms of the Landau-Zener-Stückelberg (LZS) transition [23–26]. Thus a minimal magnetic model Hamiltonian should contain (strong) Heisenberg interactions, the single-ion anisotropy, the DMI and a coupling to the applied magnetic field [10, 34–42]. As the DMI mixes states with different magnetization, it is not possible to use the magnetization as a vehicle to block-diagonalize the Hamiltonian and effectively reduce the size of the matrices that have to be diagonalized. Therefore it is of interest to explore alternative routes to direct but accurate diagonalization of the full model Hamiltonian.

We have tested different standard algorithms to compute the low-lying eigenvalues of large matrices. The standard Lanczos method (including its conjugate gradient version) as well as the power method [47, 48] either converge too slowly, lack the accuracy to resolve the (nearly)-degenerate eigen-

* Corresponding author: e-mail: deraedt@phys.rug.nl, Phone: +31 50 363 4950, Fax: +31 50 363 4947

values, and sometimes even completely fail to correctly reproduce the low-lying part of the spectrum. It seems that model Hamiltonians for nanoscale magnets provide a class of Hermitian eigenvalue problems that are hard to solve. Extensive tests lead us to the conclusion that only the Lanczos method with full orthogonalization (LFO) [47, 48] and a Chebyshev-polynomial-based projector method (CP) [49] can solve these rather large and difficult eigenvalue problems with sufficient accuracy [49].

2 Manganese complex: Mn₁₂

In the Mn₁₂-acetate molecule the four inner Mn⁺⁴ ions have spin $S = 3/2$, the other eight Mn⁺³ ions have spin $S = 2$. The number of different spin states of this system is $4^4 \times 5^8 = 10^8$. If the total magnetization is a conserved quantity, it can be used to block-diagonalize the Hamiltonian, allowing the study of models of this size [39, 43]. However, to study the adiabatic change of magnetization, we have to treat all the states, and the dimension of the matrix becomes prohibitively large. A drastic reduction of the dimension of the matrix can be achieved by approximating the magnetic moment of an inner ion by an effective $S = 1/2$ moment. The schematic diagram of this simplified (but still complicated) model is shown in Fig. 1. The number of different spin states of this model is $2^4 \times 5^4 = 10^4$. The Hamiltonian for the magnetic interactions of the simplified Mn₁₂ model can be written as [34]

$$\mathcal{H} = -J \left(\sum_{i=1}^4 S_{2i-1} \right)^2 - J' \sum_{\langle i,j \rangle} S_{2i-1} \cdot S_{2j} - K_z \sum_{i=1}^4 (S_{2i}^z)^2 + \sum_{\langle i,j \rangle} \mathbf{D}^{i,j} \cdot [S_{2i-1} \times S_{2j}] - \sum_{i=1}^8 \mathbf{h} \cdot \mathbf{S}_i, \quad (1)$$

where even (odd) numbered \mathbf{S}_i are the spin operators for the outer (inner) $S = 2$ ($S = 1/2$) spins. The first two terms describe the isotropic Heisenberg exchange between the spins. The third term describes the single-ion easy-axis anisotropy of $S = 2$ spins. The fourth term represents the antisymmetric DMI in Mn₁₂. The vector $\mathbf{D}^{i,j}$ determines the DMI between the i -th $S = 1/2$ spin and the j -th $S = 2$ spin. We do not consider higher-order correction terms that restore the SU(2) symmetry [29–31, 44]. The last term describes the interaction of the spins with the external field \mathbf{h} . Note that the factor $g\mu_B$ is absorbed in our definition of \mathbf{h} . The first three terms in Hamiltonian (1) conserve the z -component of the total spin $M^z = \sum_{i=1}^8 S_i^z$. The DMI on the other hand mixes states with different total spin and also states with the same total spin. Hence, the DMI can change level crossings into level repulsions and may explain the experimentally observed adiabatic changes of the magnetization.

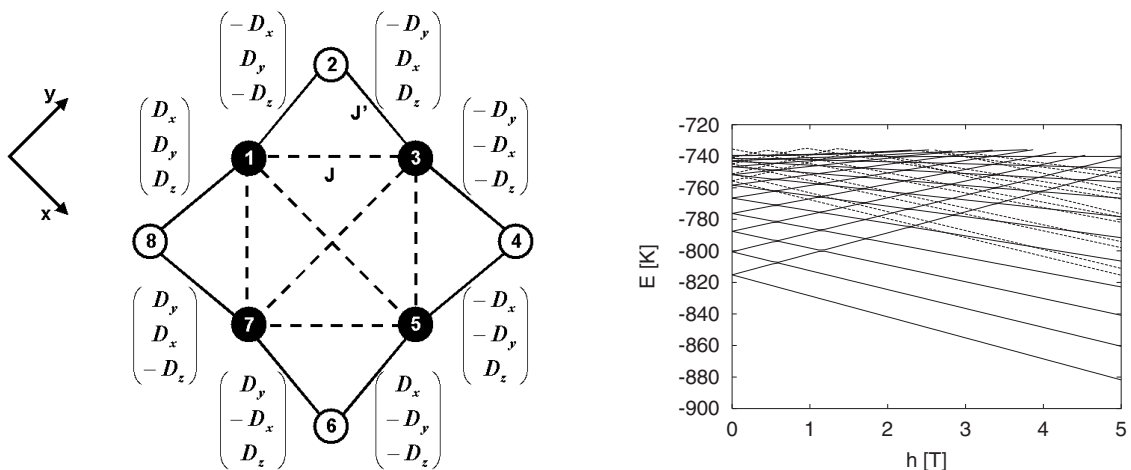


Fig. 1 Left: Schematic diagram of the magnetic interactions of the simplified model (1) of the Mn₁₂ molecule. Right: The lowest 21 energy levels of the Mn₁₂ model (1) as a function of the applied magnetic field \mathbf{h} . Solid lines: eigenstates with $|M^z| \approx 10$; dashed lines: eigenstates with $|M^z| \approx 9$.

The four-fold rotational-reflection symmetry (S_4) of the Mn_{12} molecule imposes some relations between the DM-vectors. It follows that there are only three independent DM-parameters: $D_x \equiv D_x^{1,8}$, $D_y \equiv D_y^{1,8}$, and $D_z \equiv D_z^{1,8}$, as indicated in Fig. 1. The above model satisfactorily describes a rather wide range of experimental data, such as the splitting of the neutron scattering peaks, results of EPR measurements and the temperature dependence of magnetic susceptibility [34]. The parameters of this model have been estimated by comparing experimental and theoretical data. In this paper we will use the parameter set B from Ref. [34, 40]: $J = 23.8$ K, $J' = 79.2$ K, $K_z = 5.72$ K, $D_x = 22$ K, $D_y = 0$, and $D_z = 10$ K. Although the amount of available data is not sufficient to fix all these parameters accurately, we expect that the general trends in the energy-level diagram will not change drastically if these parameters change relatively little.

Model (1) provides a good test case for diagonalization methods because it is small enough to be treated by full exact diagonalization but has all features of the larger problem. We find that the results obtained by full exact diagonalization, LFO and CP are the same to working precision (about 13 digits). For one set of model parameters, full exact diagonalization (using standard LAPACK algorithms) of the 10000×10000 matrix representing model (1) takes about 2 hours of CPU time on an Athlon 1.8 GHz/1.5Gb system. In Fig. 1 we show the results, obtained by LFO, for the lowest 21 energy levels of the Mn_{12} model as a function of the applied magnetic field. For each value of the h -field, the LFO calculation takes about 20 minutes and uses much less memory than the full diagonalization method.

Although the total magnetization is not a good quantum number, we can label the various eigenstates by their (calculated) magnetization. For large fields and/or energies, eigenstates with total spin 8, 9 and 10 appear. In Fig. 1 eigenstates with $|M^z| \approx 10(9)$ (within an error of about 10%) are represented by solid (dashed) lines (eigenstates with $|M^z| \approx 8$ appear for $h > 4$ but have been omitted for clarity). The standard $S = 10$ single-spin model for Mn_{12} , $\mathcal{H} = -D(S^z)^2 - hS^z$, is often used as a starting point to interpret experimental results [6, 7, 11–13, 37]. The energy levels of this model exhibit crossings at the resonant fields $h = \pm Dn$ for $n = -10, \dots, 10$, in agreement with our numerical results for the more microscopic model (1). For the parameter set B, we find that $D \approx 0.55K$, in good agreement with experiments [6, 7]. The single-spin model commutes with the magnetization S^z and therefore it only displays level crossings, no level repulsions. Adding an anisotropy term of the form $S_+^4 + S_-^4$ only leads to level repulsions when the magnetization changes by 4, which does not agree with the observation of adiabatic changes of the magnetization for all $h = nD$ [6, 7, 11, 12]. In contrast, for the DMI the Hamiltonian has nonzero matrix elements for the pairs of states $|S, S_z\rangle$ and $|S \pm 1, S_z \pm 1\rangle$, but zero matrix elements for levels with the same value of the total spin.

In Fig. 1, for some values of h , level repulsions appear to be present. However, these are due to the fitting procedure used to plot the data and the number of h -values used (100) and disappear by using a higher resolution in h -fields (results not shown). Thus these splittings have no physical meaning. For the Mn_{12} system, the energy splittings at low field are extremely small. Their calculation requires extended-precision (128-bit) arithmetic [40]. Adding an extra transverse field by tilting the h -field by 5 degrees does not change this conclusion. Thus, it is clear that within the (very high) resolution in the h -field and the 13-digit precision of the calculation, there is no compelling evidence that the DMI gives rise to a level repulsion, at least not for the choice of model parameters (set B, see above) considered here. The algorithms developed for the work presented in this paper can be used for 33-digit calculations without modification and we leave the calculation of the splittings for future work.

3 Vanadium complex: V_{15}

In Fig. 2 we show the schematic diagram of the dominant magnetic (Heisenberg) interactions of the V_{15} molecule. The magnetic structure consists of two hexagons with six $S = 1/2$ spins each, enclosing a triangle with three $S = 1/2$ spins. All dominant Heisenberg interactions are antiferromagnetic. The number of different spin states of this model is $2^{15} = 32768$. The minimal Hamiltonian for the

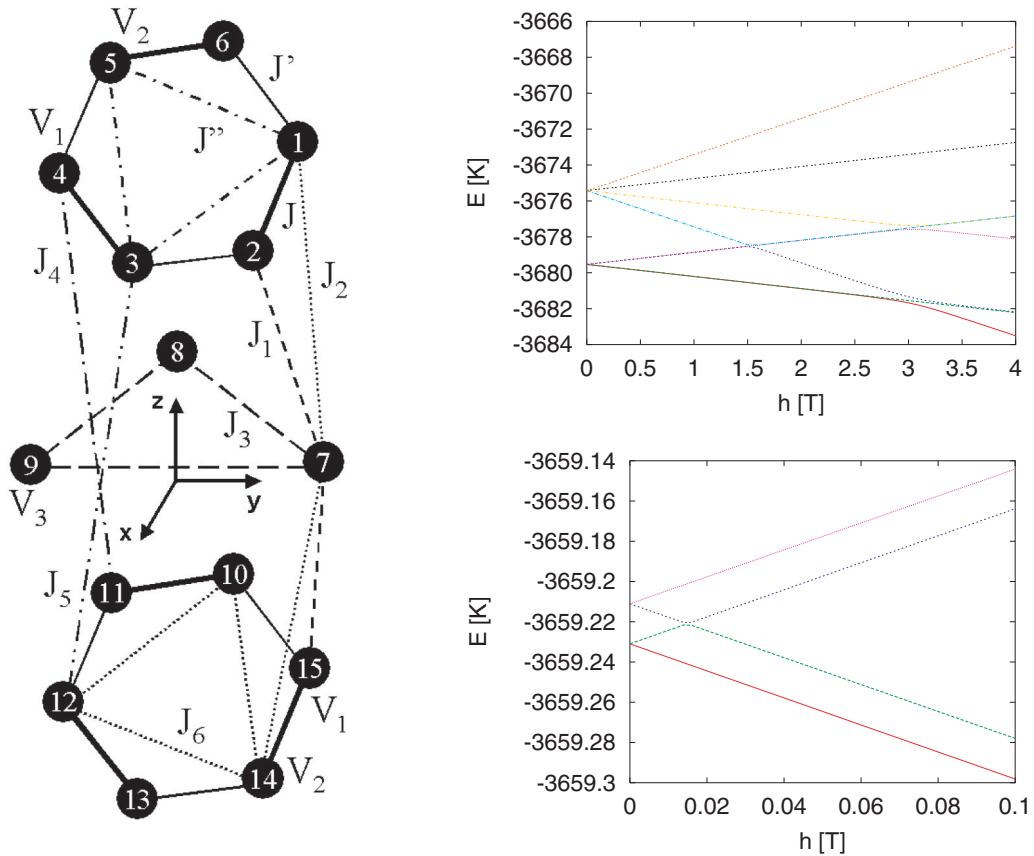


Fig. 2 (online colour at: www.interscience.wiley.com) Left: Schematic diagram of the magnetic interactions in model (2) of the V_{15} molecule. Right top: The lowest 8 energy levels of V_{15} model (2) with model parameters taken from Ref. [42] as a function of the applied magnetic field h parallel to the z -axis. Right bottom: Detailed view of the four lowest energy levels at $h \approx 0$.

magnetic interactions that incorporates the effects on magnetic anisotropy can be written as [22, 37, 38, 41]

$$\mathcal{H} = -\sum_{\langle i,j \rangle} J_{i,j} \mathbf{S}_i \cdot \mathbf{S}_j + \sum_{\langle i,j \rangle} \mathbf{D}^{i,j} \cdot [\mathbf{S}_i \times \mathbf{S}_j] - \sum_i \mathbf{h} \cdot \mathbf{S}_i. \quad (2)$$

The various Heisenberg interactions $J_{i,j}$ are shown in Fig. 2. For simplicity, we assume that $\mathbf{D}^{i,j} = 0$ for sites i and j except for bonds for which the Heisenberg exchange constant is J (see Fig. 2) [37, 41]. Rotations about $2\pi/3$ and $4\pi/3$ around the axis perpendicular to and passing through the center of the hexagons leave the V_{15} complex invariant. This enforces constraints on the values of $\mathbf{D}^{i,j}$ [41, 42]. We have calculated the energy level diagram for the sets of model parameters given in Refs. [18], [37], and [41]. The level diagrams for these three choices are qualitatively similar [49]. Therefore we only present results for one set of model parameters.

Following Ref. [37] we take $J = -800$, $J_1 = J' = -54.4$ K, and $J_2 = J'' = -160$ K, $J_3 = J_4 = J_5 = J_6 = 0$. Then, in the absence of the DMI, we find for the energy gap between the ground state and the first excited state at $h = 0$ a value of 4.12478 K, in perfect agreement with Ref. [37]. As in Ref. [42] we take for the DMI parameters $D_x^{1,2} = D_y^{1,2} = D_z^{1,2} = 40$ K in the present lattice (Fig. 2). The amplitude is approximately 5% of the largest Heisenberg coupling. Using the rotational symmetry of the hexagon we have $D_x^{3,4} = 14.641$ K, $D_y^{3,4} = -54.641$ K, $D_z^{3,4} = 40$ K and $D_x^{5,6} = -54.641$ K, $D_y^{5,6} = 14.641$ K, $D_z^{5,6} = 40$ K. As the two hexagons are not equivalent we cannot use symmetry to

reduce the number of free parameters. For simplicity, we assume that the (x, y) positions of the spins on the lower hexagons differ from those on the upper hexagon by a rotation about $\pi/3$. This yields for the remaining model parameters $D_x^{10,11} = -14.641$ K, $D_y^{10,11} = 54.641$ K, $D_z^{10,11} = 40$ K, $D_x^{12,13} = -40$ K, $D_y^{12,13} = -40$ K, $D_z^{12,13} = 40$ K, and $D_x^{14,15} = 54.641$ K, $D_y^{14,15} = -14.641$ K, $D_z^{14,15} = 40$ K.

In Fig. 2 we show the results for the eight lowest energy levels of V_{15} model (2) as a function of the applied magnetic field along the z -axis, using the parameters of Ref. [42]. At zero field, the DMI splits the doubly-degenerate doublet of $S = 1/2$ states into two doublets of $S = 1/2$ states. The difference in energy of the splitting is ≈ 0.0085 K, much smaller than the experimental estimate ≈ 0.05 K [22], but of the same order of magnitude as the values cited in Ref. [41]. The next four higher levels are $S = 3/2$ states. The energy-level splitting between the $S = 3/2$ and $S = 1/2$ states is ≈ 4.1 K, in reasonable agreement with the experimental value ≈ 3.7 K [45]. The transition between the states $|1/2, 1/2\rangle$ and $|3/2, 3/2\rangle$ takes place at $h \approx 2.8$ T in very good agreement with the experimental value 2.8 T. It should be noted that an energy gap does not necessarily implies an energy-level repulsion, as Fig. 2 demonstrates for the case when the magnetic field is applied in the z direction. Here we find that the levels simply cross at a finite value of the field, and the system does not allow for an adiabatic change of the magnetization between the states $|1/2, -1/2\rangle$ and $|1/2, 1/2\rangle$. If we apply the field in the x or y direction, the energy-level diagram exhibits degenerate repulsions as shown in Ref. [22]. If we apply in an intermediate angle, the energy structure changes smoothly from that for z direction to that for x (or y) direction. Therefore, although the DMI causes the avoided level crossing structure, it is anisotropic with respect to the direction of the field. This structure (by a factor of two at least) should lead to observable changes in the hysteresis loops but has not been seen in experiment [45]. Our numerical data for the model parameters given in Refs. [18], [37], and [41] suggest that the three-spin model reproduces the main features of the full V_{15} model. Within the three spin model we have studied the effects of higher-order correction terms that restore the $SU(2)$ symmetry [29–31, 44]. While they cause the four $S = 3/2$ levels to be degenerate at $h = 0$, the low energy degenerate doublets do not change in an essential manner. In experiments only weak directional dependence was found. Thus, it seems that another type of mechanism for opening gaps is at work and, as we have shown elsewhere, hyperfine interactions seems to be a good candidate [50].

Acknowledgements We thank I. Chiorescu, and V. Dobrovitski for illuminating discussions. Support from the ‘Nederlandse Stichting voor Nationale Computer Faciliteiten (NCF)’ is gratefully acknowledged.

References

- [1] L. Gunther and B. Barbara (Eds.), *Quantum Tunneling of Magnetization*, NATO ASI Ser. E, Vol. 301 (Kluwer, Dordrecht, 1995).
- [2] A. Caneschi, D. Gatteschi, R. Sessoli, A. Barra, L. C. Brunel, and M. Guillot, *J. Am. Chem. Soc.* **113**, 5873 (1991).
- [3] R. Sessoli, H.-L. Tsai, A. R. Shake, S. Wang, J. B. Vincent, K. Folting, D. Gatteschi, G. Christou, and D. N. Hendrickson, *J. Am. Chem. Soc.* **115**, 1804 (1993).
- [4] D. Gatteschi, L. Pardi, A. L. Barra, and A. Müller, *Mol. Eng.* **3**, 157 (1991).
- [5] G. Levine and J. Howard, *Phys. Rev. Lett.* **75**, 4142 (1995).
- [6] J. R. Friedman, M. P. Sarachik, J. Tejada, and R. Ziolo, *Phys. Rev. Lett.* **76**, 3830 (1996).
- [7] L. Thomas, F. Lioni, R. Ballou, D. Gatteschi, R. Sessoli, and B. Barbara, *Nature* **383**, 145 (1996).
- [8] C. Sangregorio, T. Ohm, C. Paulsen, R. Sessoli, and D. Gatteschi, *Phys. Rev. Lett.* **78**, 4645 (1997).
- [9] W. Wernsdorfer and R. Sessoli, *Science* **284**, 133 (1999).
W. Wernsdorfer, T. Ohm, C. Sangregorio, R. Sessoli, D. Mailly, and C. Paulsen, *Phys. Rev. Lett.* **82**, 3903 (1999).
- [10] B. Barbara, L. Thomas, F. Lioni, A. Sulpice, and A. Caneschi, *J. Magn. Magn. Mater.* **177**, 1324 (1998).
- [11] J. A. A. J. Perenboom, J. S. Brooks, S. Hill, T. Hathaway, and N. S. Dalal, *Phys. Rev. B* **58**, 330 (1998).
- [12] I. Chiorescu, W. Wernsdorfer, A. Müller, H. Bögge, and B. Barbara, *Phys. Rev. Lett.* **84**, 3454 (2000).
- [13] T. Pohjola and H. Schoeller, *Phys. Rev. B* **62**, 15026 (2000).

- [14] Y. Zhong, M. P. Sarachik, J. Yoo, and D. N. Hendrickson, *Phys. Rev. B* **62**, R9256 (2000).
- [15] I. Chiorescu, W. Wernsdorfer, A. Müller, H. Bögge, and B. Barbara, *J. Magn. Magn. Mater.* **221**, 103 (2000).
- [16] I. Chiorescu, W. Wernsdorfer, A. Müller, H. Bögge, and B. Barbara, *Phys. Rev. Lett.* **84**, 3454 (2000).
- [17] I. Chiorescu, R. Giraud, A. G. M. Jansen, A. Caneschi, and B. Barbara, *Phys. Rev. Lett.* **85**, 4807 (2000).
- [18] D. W. Boukhvalov, V. V. Dobrovitski, M. I. Katsnelson, A. I. Lichtenstein, B. N. Harmon, and P. Kögerler, *J. Appl. Phys.* **93**, 7082 (2003).
- [19] D. W. Boukhvalov, A. I. Lichtenstein, V. V. Dobrovitski, M. I. Katsnelson, B. N. Harmon, V. V. Mazurenko, and V. I. Anisimov, arXiv:cond-mat/0110488.
- [20] W. Wernsdorfer, N. Allaga-Alcalde, D. N. Hendrickson, and G. Christou, *Nature* **416**, 407 (2002).
- [21] A. Honecker, F. Meier, D. Loss, and B. Normand, *Eur. Phys. J. B* **27**, 487 (2002).
- [22] I. Chiorescu, W. Wernsdorfer, A. Müller, S. Miyashita, and B. Barbara, arXiv: cond-mat/0212181.
- [23] S. Miyashita, *J. Phys. Soc. Jpn.* **64**, 3207 (1997); *ibid.* **65**, 2734 (1996).
- [24] V. V. Dobrovitskii and A. K. Zvezdin, *Europhys. Lett.* **38**, 377 (1997).
- [25] L. Gunther, *Europhys. Lett.* **39**, 1 (1997).
- [26] H. De Raedt, S. Miyashita, K. Saitoh, D. García-Pablos, and N. García, *Phys. Rev. B* **56**, 11761 (1997).
- [27] I. E. Dzyaloshinskii, *Zh. Eksp. Teor. Fiz.* **32**, 1547 (1957) [*Sov. Phys. – JETP* **5**, 1259 (1957)].
- [28] T. Moriya, *Phys. Rev.* **120**, 91 (1960).
- [29] T. A. Kaplan, *Z. Phys. B* **49**, 313 (1983).
- [30] L. Shekhtman, O. Entin-Wohlman, and A. Aharony, *Phys. Rev. Lett.* **69**, 836 (1992).
- [31] L. Shekhtman, A. Aharony, and O. Entin-Wohlman, *Phys. Rev. B* **47**, 174 (1993).
- [32] K. Yosida, *Theory of Magnetism* (Springer-Verlag, Berlin, New York, 1996).
- [33] A. Crépieux and C. Lacroix, *J. Magn. Magn. Mater.* **182**, 341 (1998).
- [34] M. I. Katsnelson, V. V. Dobrovitski, and B. N. Harmon, *Phys. Rev. B* **59**, 6919 (1999).
- [35] M. Al-Saquer, V. V. Dobrovitski, B. N. Harmon, and M. I. Katsnelson, *J. Appl. Phys.* **87**, 6268 (2000).
- [36] I. Rudra, S. Ramasesha, and D. Sen, *Phys. Rev. B* **64**, 014408 (2001).
- [37] I. Rudra, S. Ramasesha, and D. Sen, *J. Phys.: Condens. Matter* **13**, 11717 (2001).
- [38] S. Miyashita and N. Nagaosa, *Prog. Theor. Phys.* **106**, 533 (2001).
- [39] C. Raghun, I. Rudra, D. Sen, and S. Ramasesha, *Phys. Rev. B* **64**, 064419 (2001).
- [40] H. De Raedt, A. H. Hams, V. V. Dobrovitsky, M. Al-Saquer, M. I. Katsnelson, and B. N. Harmon, *J. Magn. Magn. Mater.* **246**, 392 (2002).
- [41] N. P. Konstantinidis and D. Coffey, *Phys. Rev. B* **66**, 174426 (2002).
- [42] I. Rudra, K. Saito, S. Ramasesha, and S. Miyashita, unpublished.
- [43] N. Regnault, Th. Jolicoeur, R. Sessoli, D. Gatteschi, and M. Verdaguer, *Phys. Rev. B* **66**, 054409 (2002).
- [44] A. Zheludev, S. Maslov, I. Tsukada, I. Zaliznyak, L. P. Regnault, T. Masuda, K. Uchinokura, R. Erwin, and G. Shirane, *Phys. Rev. Lett.* **81**, 5410 (1998).
- [45] I. Chiorescu, private communication
- [46] V. V. Kostyuchenko and A. K. Zvezdin, *Phys. Solid State* **45**, 903 (2003).
- [47] J. H. Wilkinson, *The Algebraic Eigenvalue Problem* (Clarendon Press, Oxford, 1965).
- [48] G. H. Golub and C. F. Van Loan, *Matrix Computations* (John Hopkins University Press, Baltimore, 1996).
- [49] H. De Raedt, S. Miyashita, and K. Michielsen, submitted to *Phys. Rev. B*, <http://arXiv.org/abs/cond-mat/0306275>.
- [50] S. Miyashita, H. De Raedt, and K. Michielsen, *Prog. Theor. Phys.* **110**, 889 (2003).